

# Supporting Information

## Can two-dimensional boron superconduct?

Evgeni S. Penev,<sup>†,‡</sup> Alex Kutana,<sup>†,‡</sup> and Boris I. Yakobson<sup>\*,†</sup>

*Department of Materials Science and NanoEngineering, Rice University, Houston, Texas 77005*

E-mail: [biy@rice.edu](mailto:biy@rice.edu)

### Methodology

All results are obtained using the PHONON module of QUANTUM ESPRESSO.<sup>1</sup> It evaluates the McMillan formula<sup>2</sup> for the critical temperature  $T_c$  for phonon-mediated superconductivity, with the  $\omega_{\text{ln}}$  prefactor modifications proposed by Allen and Dynes,<sup>3</sup>

$$k_B T_c = \frac{\hbar \omega_{\text{ln}}}{1.2} \exp\left(-\frac{1.04(1+\lambda)}{\lambda - \mu^* - 0.62\lambda\mu^*}\right). \quad (\text{S1})$$

All  $T_c$  values reported in the main text are obtained with Coulomb pseudopotential  $\mu^* = 0.1$ , and Figure S1 illustrates the range of  $T_c$  variation with  $\mu^*$ . The calculation of the electron-phonon coupling constant  $\lambda$  is based on density-functional perturbation theory,<sup>4</sup> according to:

$$\lambda = \int_{\text{BZ}} \frac{d\mathbf{k}}{\Omega_{\text{BZ}}} \lambda_{\mathbf{k}}, \quad (\text{S2})$$

where  $\Omega_{\text{BZ}}$  is the BZ “volume”, and we have defined the  $\mathbf{k}$ -resolved coupling as

$$\lambda_{\mathbf{k}} = \frac{2}{N(\varepsilon_F)} \frac{1}{2M} \int_{\text{BZ}} \frac{d\mathbf{q}}{\Omega_{\text{BZ}}} \sum_{\nu} \frac{1}{\omega_{\mathbf{q}\nu}^2} \sum_{ij} \delta(\varepsilon_{i\mathbf{k}} - \varepsilon_F) \times \delta(\varepsilon_{j\mathbf{k}+\mathbf{q}} - \varepsilon_F) \left| \left\langle \psi_{i\mathbf{k}} \left| \boldsymbol{\epsilon}_{\mathbf{q}\nu} \cdot \nabla V \right| \psi_{j\mathbf{k}+\mathbf{q}} \right\rangle \right|^2. \quad (\text{S3})$$

\*To whom correspondence should be addressed

<sup>†</sup>Department of Materials Science and NanoEngineering, Rice University, Houston, Texas 77005

<sup>‡</sup>These authors contributed equally to this work.

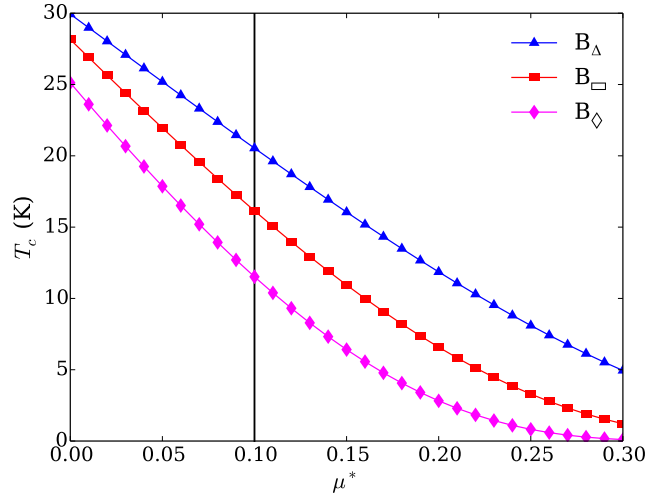


Figure S1: Critical temperature  $T_c$  as given by the McMillan equation S1 as a function of the empirical parameter  $\mu^*$  for  $B_{\Delta}$ ,  $B_{\square}$ , and  $B_{\diamond}$  boron structures. Vertical line marks the value  $\mu^* = 0.1$  used in this work.

In the above equation  $\omega_{\mathbf{q}\nu}$  is the frequency of the phonon mode  $(\mathbf{q}, \nu)$ , and  $\boldsymbol{\epsilon}_{\mathbf{q}\nu}$  – its polarization vector, and  $V$  – the self-consistent potential.

In the  $\mathbf{q}$ -space, we plot  $\lambda_{\mathbf{q}\nu}$ , defined as

$$\lambda_{\mathbf{q}\nu} = \frac{1}{N(\varepsilon_F) M \omega_{\mathbf{q}\nu}^2} \int_{\text{BZ}} \frac{d\mathbf{k}}{\Omega_{\text{BZ}}} \sum_{ij} \delta(\varepsilon_{i\mathbf{k}} - \varepsilon_F) \times \delta(\varepsilon_{j\mathbf{k}+\mathbf{q}} - \varepsilon_F) \left| \left\langle \psi_{i\mathbf{k}} \left| \boldsymbol{\epsilon}_{\mathbf{q}\nu} \cdot \nabla V \right| \psi_{j\mathbf{k}+\mathbf{q}} \right\rangle \right|^2, \quad (\text{S4})$$

and

$$\lambda = \sum_{\nu} \int_{\text{BZ}} \frac{d\mathbf{q}}{\Omega_{\text{BZ}}} \lambda_{\mathbf{q}\nu}. \quad (\text{S5})$$

The Eliashberg spectral function  $\alpha^2 F(\omega)$  is

Table S1: Convergence test for the triangular  $B_{\Delta}$  lattice, Figure 1a.

k-mesh	q-mesh	$\omega_{\text{ln}}$ [K]	$\lambda$	$T_c$ [K]
$64 \times 32$	$16 \times 16$	144.8	2.01	20.9
$64 \times 32$	$32 \times 32$	197.0	1.37	20.5
$64 \times 32$	$64 \times 32$	238.1	1.18	21.0
$128 \times 64$	$128 \times 64$	272.5	1.05	20.5

given by:

$$\alpha^2 F(\omega) = \frac{1}{2} \sum_{\nu} \int_{\text{BZ}} \frac{d\mathbf{q}}{\Omega_{\text{BZ}}} \lambda_{\mathbf{q}\nu} \omega_{\mathbf{q}\nu} \delta(\omega - \omega_{\mathbf{q}\nu}). \quad (\text{S6})$$

The frequency  $\omega_{\text{ln}}$  is defined as

$$\omega_{\text{ln}} = \exp\left(\frac{2}{\lambda} \int_0^{\infty} \alpha^2 F(\omega) \frac{\ln \omega}{\omega} d\omega\right), \quad (\text{S7})$$

where  $\lambda \equiv \lambda(\omega \rightarrow \infty)$ , and

$$\lambda(\omega) = 2 \int_0^{\omega} \frac{\alpha^2 F(\omega')}{\omega'} d\omega'. \quad (\text{S8})$$

Methfessel–Paxton smearing with width of 1 meV was used to obtain  $\alpha^2 F(\omega)$  and  $\lambda$ .

## Density of states, Fermi surface, and phonon dispersions

Projected density of states  $N_l(\varepsilon)$  in Figures 2a, 4a, and 6a, were calculated using the following input group

```
&projwfc
...
DeltaE = 0.01
ngauss = 1
degauss = 0.01
lsym = .true.
...
/
```

and, as in our previous work Ref.,<sup>5</sup>

$$N_{s+p_x, y}(\varepsilon) \equiv \sum_{l=s, p_x, p_y} N_l(\varepsilon). \quad (\text{S9})$$

Fermi contours were obtained using MATHEMATICA to solve for  $\mathbf{k}$ , and all  $i$ , such that  $\varepsilon_{i\mathbf{k}} =$

Table S2: Convergence test for the rectangular structure  $B_{\square}$ , Figure 1b.

k-mesh	q-mesh	$\omega_{\text{ln}}$ [K]	$\lambda$	$T_c$ [K]
$64 \times 32$	$8 \times 8$	343.2	0.812	16.6
$64 \times 32$	$16 \times 16$	362.0	0.785	16.3
$64 \times 32$	$32 \times 32$	361.8	0.781	16.1
$64 \times 32$	$64 \times 32$	362.0	0.781	16.1

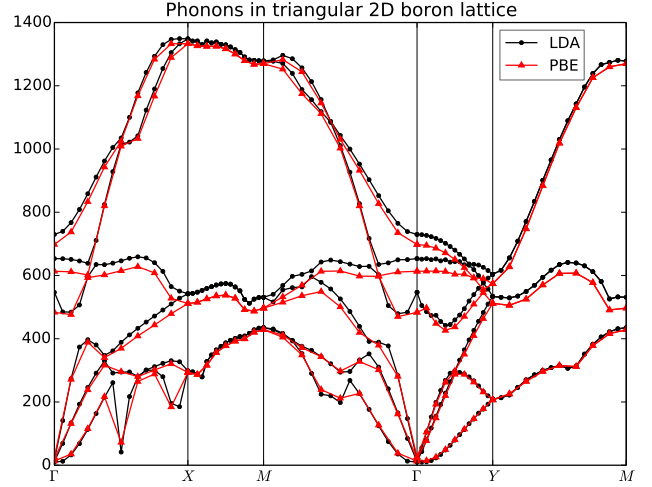


Figure S2: Comparison of LDA and PBE phonon dispersions in triangular structure  $B_{\Delta}$  obtained using a  $64 \times 32$  k-point grid and  $32 \times 32$  (LDA),  $16 \times 16$  (PBE) q-point grids.

$\varepsilon_{\mathbf{F}} \equiv \text{const}$ , with eigenvalues  $\varepsilon_{i\mathbf{k}}$  calculated in the entire BZ, following similar protocol as in the case of a band structure calculation with QUANTUM ESPRESSO.

All results reported in the main text are based on the following production-quality, identical k- and q-point meshes:  $128 \times 64$  for the  $B_{\Delta}$  structure,  $64 \times 32$  for the  $B_{\square}$  structure, and  $64 \times 64$  for the  $B_{\diamond}$  structure. This choice ensures converged results for the electronic structures and phonons and is made on the basis of the benchmarks compiled in Tables S1–S3. These meshes are automatically generated, e.g.,

```
K_POINTS automatic
128 64 1 0 0 0
```

and result in 2145, 561, and 1057 k- and q-points in the irreducible wedge of the BZ (shaded areas in Figure 2b, Figure 4b, and Figure 6b) of each structure, respectively. This corresponds to a density of sampling points which is at least  $160/2\pi \text{ \AA}$  along each axis in reciprocal space in all cases.

Table S3: Convergence test for the  $c$ -rectangular structure  $B_{\diamond}$ , Figure 1c.

k-mesh	q-mesh	$\omega_{\text{in}}$ [K]	$\lambda$	$T_c$ [K]
$64 \times 64$	$16 \times 16$	479.7	0.59	10.4
$64 \times 64$	$32 \times 32$	440.2	0.63	11.8
$64 \times 64$	$64 \times 64$	455.4	0.62	11.5

Table S4: Variation of calculated  $T_c$  with Gaussian smearing width  $\sigma$ .

$\sigma$ [Ry]	$T_c$ [K]		
	$B_{\Delta}$	$B_{\square}$	$B_{\diamond}$
0.005	19.782	26.463	13.337
0.010	20.521	22.169	13.545
0.015	20.683	18.560	12.551
0.020	20.536	16.144	11.520
0.025	20.352	14.475	10.638
0.030	20.216	13.286	9.915
0.035	20.134	12.426	9.336
0.040	20.070	11.799	8.873
0.045	19.984	11.340	8.498
0.050	19.853	11.000	8.183

Dense k-point mesh is required because of metallicity, while dense q-point mesh is necessary due to the long-range nature of force constants in these materials. The plane wave cutoff energy of 70 Ry was used to represent wavefunctions, and 280 Ry to represent charge density in all calculations.

Figure S2 shows a single calculation carried out with the PBE functional, using coarser grids, to test for possible differences due to using generalized gradient approximation (GGA) for the electronic exchange and correlation. Comparison of the phonon dispersions along  $\Gamma$ -X to those in Figure 3 in the main text shows that Kohn anomalies cannot be resolved with the coarser meshes in Table S1.

The effect of Gaussian smearing width used for integration over the 2D Fermi contour in calculating the electron-phonon coupling coefficients  $\lambda_{q\nu}$ , for determining the Fermi level  $\varepsilon_F$ , the corresponding total electronic density of states  $N(\varepsilon_F)$ , and to calculate the isotropic Eliashberg spectral function  $\alpha^2F(\omega)$  is given in Table S4. The shaded row is the representative set reported in the main text.

Figures S3 and S4 demonstrate the removal (by small tensile strain) of the small imaginary  $\omega_q^2 < 0$  which are found for the relaxed geometries of the

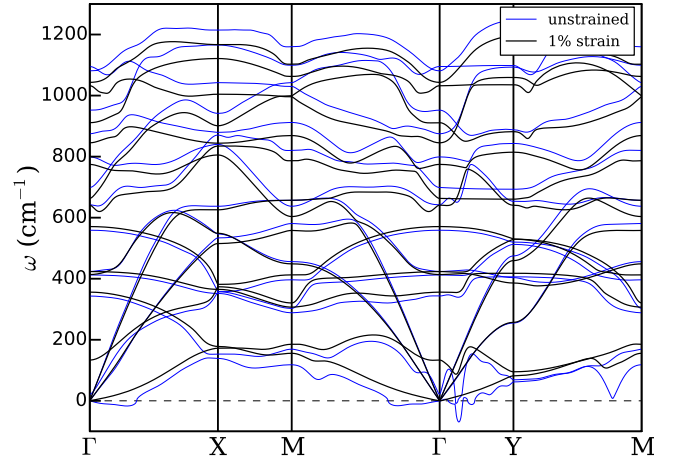


Figure S3: Phonon spectra of the  $B_{\square}$  2D boron structure with 0% and 1% in-plane tensile strain obtained using  $16 \times 16$  and  $64 \times 32$  q-point grids, respectively.

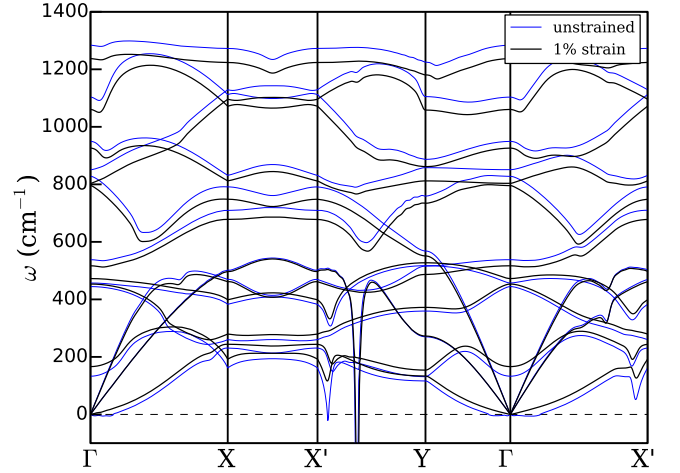


Figure S4: Phonon spectra of the  $B_{\diamond}$  2D boron structure with 0% and 1% in-plane tensile strain obtained using a  $64 \times 64$  q-point grid.

$B_{\square}$  and  $B_{\diamond}$  lattices in vicinity of the BZ center.

## References

- (1) Giannozzi, P.; Baroni, S.; Bonini, N.; Calandra, M.; Car, R.; Cavazzoni, C.; Ceresoli, D.; Chiarotti, G. L.; Cococcioni, M.; Dabo, I.; Corso, A. D.; de Gironcoli, S.; Fabris, S.; Fratesi, G.; Gebauer, R.; Gerstmann, U.; Gougoussis, C.; Kokalj, A.; Lazzeri, M.; Martin-Samos, L.; Marzari, N.; Mauri, F.; Mazzarello, R.; Paolini, S.; Pasquarello, A.; Paulatto, L.; Sbraccia, C.; Scandolo, S.; Sclauzero, G.; Seitsonen, A. P.; Smogunov, A.; Umari, P.; Wentzcovitch, R. M.

QUANTUM ESPRESSO: a modular and open-source software project for quantum simulations of materials. *J. Phys.: Condens. Matter* **2009**, *21*, 395502.

- (2) McMillan, W. L. Transition Temperature of Strong-Coupled Superconductors. *Phys. Rev.* **1968**, *167*, 331–344.
- (3) Allen, P. B.; Dynes, R. C. Transition temperature of strong-coupled superconductors reanalyzed. *Phys. Rev. B* **1975**, *12*, 905–922.
- (4) Baroni, S.; de Gironcoli, S.; Dal Corso, A.; Giannozzi, P. Phonons and related crystal properties from density-functional perturbation theory. *Rev. Mod. Phys.* **2001**, *73*, 515–562.
- (5) Penev, E. S.; Bhowmick, S.; Sadrzadeh, A.; Yakobson, B. I. Polymorphism of Two-Dimensional Boron. *Nano Lett.* **2012**, *12*, 2441–2445.